

Chapter 7

Characterization Techniques for Electrochemical Analysis



Euth Ortiz Ortega, Hamed Hosseinian, Ingrid Berenice Aguilar Meza, Andrea Rodríguez Vera, María José Rosales López, and Samira Hosseini

Abbreviations

AC	Alternating current
Ag ⁺	Silver ions
AMF	Autocrine motility factor
Au	Gold
AuNPs	Gold nanoparticles
BSA	Bovine serum albumin
C	Capacitance
CDMPV	Cyclic differential multipulse voltammetry
CE	Counter electrode
CEA	Carcinoembryonic antigen
CMPV	Cyclic multipulse voltammetry
CNTs	Carbon nanotubes
CSs	Microcarbon sphere
Cu-Au	Copper-gold
CV	Cyclic voltammetry
DA	Dopamine
DC	Direct current
DHF	Dengue hemorrhagic fever
DME	Dropping mercury electrode
DSS	Dengue shock syndrome
$E(t)$	Sinusoidal perturbations of potential
E_0	Amplitude of potential
EIS	Electrochemical impedance spectroscopy
ELLI	Electro-lateral flow immunosensor
E_p	Peak potential
E_{pa}	Peak anodic potential
E_{pc}	Peak cathodic potential

FAR	Folate receptor
FRA	Frequency response analyzer
FSCV	Fast-scan cyclic voltammetry
H ₂ SO ₄	Sulfuric acid
$I(t)$	Sinusoidal current
I_0	Amplitude of current
i_{pa}	Anodic current
i_{pc}	Cathodic current
K ₄ [Fe (CN) ₆]	Potassium ferricyanide
LTS	Linear systems theory
LOD	Limit of detection
MUA	Mercaptoundecanoic acid
PEG	Polyethylene glycol
PGI	Phosphoglucose isomerase
RE	Reference electrode
R_{et}	Resistance to electron transfer
R_s	Resistance to the solution
SNR	Signal-to-noise ratio
SPGE	Screen-printed gold electrodes
SWNTs	Single-walled carbon nanotubes
UiO-66	Zirconium MOFs
V_1	Potential 1
V_2	Potential 2
WE	Working electrode
Z	Electrochemical impedance of electrode reaction
Z_w	Warburg impedance
ϕ	Phase shift
ω	Frequency
Ω	Ohms

7.1 Cyclic Voltammetry for Material Characterization

7.1.1 History of Cyclic Voltammetry

Cyclic voltammetry (CV) is an electroanalytical method which obtains qualitative information about electrochemical reactions by measuring the flow of current between electrodes. These are presented as current–voltage curves, also called voltammograms. In order to discuss this method, some concepts must first be introduced [1, 2]. Among the given concepts that were established for the development of electro-analysis were the fundamentals of electrolysis initiated by the discovery of Alessandro Volta’s pile in 1800 (Fig. 7.1). A year later, in 1801, William Cruikshank

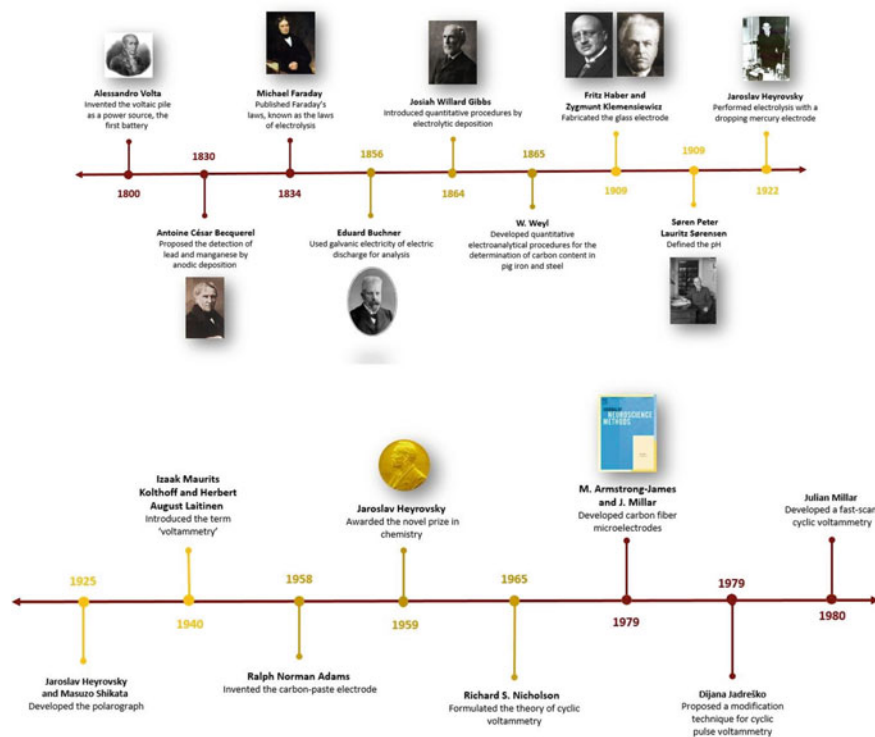


Fig. 7.1 History of CV from its beginning with the invention of the “voltaic pile” in 1800 until 1980, when Millar developed the fast-scan CV

suggested that current could be used as a parameter in the analysis of metals after having worked with electrolysis of aqueous solutions containing copper salts. In 1830, Antoine César Becquerel proposed the use of anodic deposition for the detection of lead and manganese. A few years later, in 1831, Michael Faraday published the laws of electrolysis. In the following decades, Eduard Buchner utilized galvanic electricity as a sensitive reagent and W. Weyl presented the mechanisms in order to identify carbon amounts in pig iron as steel after the iron electrolytic dissolution. However, quantitative electroanalytical determinations were only presented after 1864 when Josiah Willard Gibbs proposed copper precipitation by electrolysis [1]. Similarly, in 1865, Carl Luckow described copper determination by electrolytic depositions; thus, electrogravimetry for metal determination surged.

At the beginning of the twentieth century, the most outstanding development of electroanalytical techniques included the achievement of Fritz Haber and Zygmunt Klemensiewicz on glass electrodes, and the pH scale by Søren Peter Lauritz Sørensen [1]. In 1922, Jaroslav Heyrovsky performed electrolysis experiments with the dropping mercury electrode (DME). It was concluded that the results regarding the nature of the reduced species could be obtained from calculating the current while varying

the electrode's potential. This coined the origin of voltammetry and became the cause of an international reputation for Heyrovsky as the father of the electroanalytical characterization [1, 2]. Three years later, Heyrovsky and Masuzo Shikata invented an automated device called polarographs for the recording of current–voltage curves. This tool was one of the first analytical instruments for electrochemical characterization of materials which, years later, was awarded Heyrovsky the Nobel Prize in Chemistry [1, 2].

The concept of voltammetry surged in 1940 when Izaak Maurits Kolthoff and Herbert August Laitinen described the measurement of current as a function of potential at a solid working electrode [1, 2]. Although the DME greatly impacted the development of voltammetry, nowadays, it is rarely used. DME was replaced by the stationary mercury electrode in the 1950s and 1960s [1, 2]. Heinz Gerischer presented the stationary mercury drop electrode in 1953, followed by Wiktor Kemula and Zenon Kublik who later introduced a hanging mercury drop electrode known as the “Kemula electrode.” However, concerns about the toxicity of mercury at the beginning of the twenty-first century promoted restrictive regulations that progressively decreased the use of these electrodes [1, 3].

The primary steps in the establishment of voltammetry were the development of a suitable pre-concentration procedure and electrodes. In 1958, Ralph Norman Adams invented the carbon-paste electrodes, starting a time of widespread implementation of carbon electrodes. This was followed by the introduction of impregnated graphite and later pyrolytic graphite and glassy carbon by Francis J. Miller and H. E. Zittel in 1963 and 1965. These solid carbon electrodes were used for studying oxidation of organic molecules. Most recently, a vast versatility of strategies for modification of different electrodes has been investigated. The category of enzyme-modified electrodes is particularly relevant to the development of sensors. Nowadays, the modification of the electrode surface is possible with submonolayer nanoparticle coverage [1, 2, 4, 5].

Investigation of electrode surface's chemical modification around 1975 permitted better comprehension on how the surfaces could be adapted to develop the required applications. Arthur Thornton Hubbard, Theodore Kuwana, Royce W. Murray, among others, made initial efforts in covalently attaching different monolayers to electrodes. In the late 1970s, Murray, along with L. L. Miller, Allen J. Bard, and co-workers, modified electrodes by creating controlled polymer layers on the electrode surface [1, 2, 4]. In 1965, Richard S. Nicholson formulated the theory of cyclic voltammetry. In spite of its complex theory, it soon became one of the prevailing electrochemical techniques. It is often employed to obtain thermodynamic and kinetic information of electroactive compounds, either organic, organometallic, or inorganic species, especially when electrochemical methods are occasionally used [2, 6].

Computers greatly influenced electrochemical instrumentation as they served to generate potential programs. Voltammetric perturbation applied to the system could now be adjusted by researchers on modern software packages in electrochemical instrumentation. Therefore, in 2013, technique variations of the cyclic pulse voltammetry were proposed. Some of these included the cyclic multipulse voltammetry (CMPV) and cyclic differential multipulse voltammetry (CDMPV), resulting in a more complete characterization of the system and sound, and faster electrochemical

calculations. The obtained signal enabled the qualitative analysis of the procedure from the visual examination of the voltammograms [2, 4]. Additionally, bulk kinetics could be used to identify authentic nano-electrocatalysis by simulating different experiments. These include voltammetry experiments on nanoparticle-modified electrodes in relation to surface coverage and voltammetry experiments on bulk material using a macroelectrode. Due to the diffusion profile being able to overlap and the complex interaction of the electrode surface geometry, the production of physically significant kinetic data from modified electrodes was a laborious drawback. Therefore, these simulation analyses could be used to conclude if the voltammetric response was experimentally adapted by the application of the nanomaterial [4]. The world is moving toward miniaturization; hence, the characterization domain is advancing toward quicker and more compact techniques, allowing voltammetry to proceed in the same manner [2]. In that path, selective reagents, electrochemical mediators, new materials, and modification strategies should be incorporated to improve the selectivity and the sensitivity of existing electrochemical sensors [3].

7.1.2 Mechanism of Operation of Cyclic Voltammetry

In order to conduct a CV experiment, some criteria must be met such as the three-electrode setup with a working electrode (WE), a reference electrode (RE), and a counter electrode (CE). To clarify this mechanism, there are some phrases that must be first defined. Reduction occurs in the electrode on the cathode, marking the cathode as the reducing electrode. A WE is an electrode where the reduction or oxidation electrochemical phenomena are taking place. CE functions as an electron source; hence, the current may flow from the external circuit through the cell. For instance, for each electron stopped at the WE by oxidation, a one-electron reduction procedure must occur at the CE. A RE is a stable electrode with a constant potential (despite the electrolyte solution it is dipped in), and it calculates the potential of the WE. An inorganic salt that is dissolved in an aqueous solution which is an ionic conductor is called an electrolyte solution. A potentiostat is an electronic amplifier designed to control the WE potential in a multiple-electrode electrochemical cell. The potentiostat usually contains a sensing component like a RE, a component for balancing the current flow like a CE, and various internal circuits that allow it to function in this capacity. By using a potentiostat and a three-electrode setup, it is possible to record a current–potential polarization curve for two purposes including: (1) having control over the voltage between the WE and the RE, and (2) calculating the flow of current between the WE and the CE.

For a bioanode, the above-mentioned is demonstrated in Fig. 7.2. This figure represents the voltage drop between the RE and the WE. This voltage drop is obtained via “R,” the resistance generated by the electrolyte located between the WE and the RE. *R* is also referred to as the uncompensated resistance. As the current flows, according to Ohm’s law, this resistance results in a decrease in potential in the solution. As the resistivity of the solution and the distance between the WE and the RE increase, the

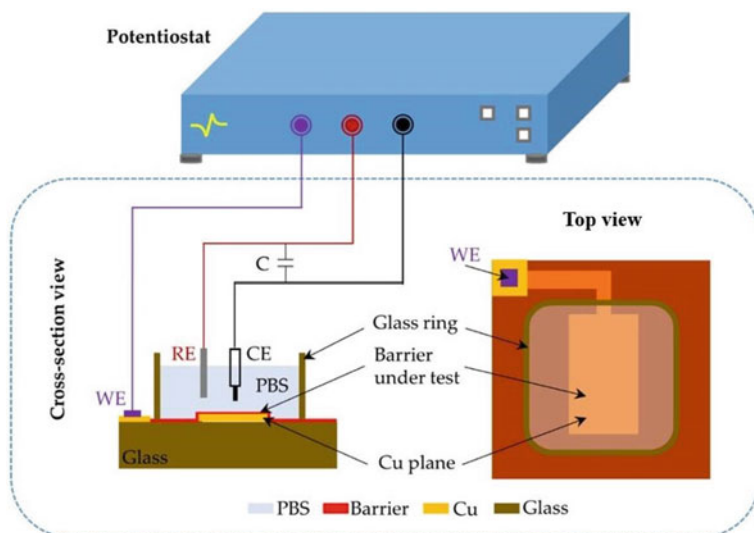


Fig. 7.2 A conventional setup with three electrodes of an electrochemical cell connected to a potentiostat

potential further decreases. Additionally, it is best to maintain the RE secluded from the ion migration between WE and CE to avoid incorrect potential measurement. In order to prevent a large decrease in potential between the WE and the RE, it is advised to position the RE and WE near each other. The effect of the uncompensated resistance, the resistance between the working electrodes, and the full equipotential surface through the tip of the reference electrode could be measured for different setups [7].

Additionally, CV can provide other relevant information such as the chemical rate constant of the redox potential and the electrochemical reaction rates. A very noticeable factor for chemical reactions to happen at a significant proportion is the scan rate which must be long enough. A current is measured between the WE and the CE, while a voltage will be measured between the RE and the WE. The voltammogram includes oxidative and reductive peaks, as is presented in Fig. 7.3 where a normal voltammogram is demonstrated to represent different peaks and components. The current rises from the capacitive or resting phase, while the applied potential hikes from Potential 1 (V_1) to Potential 2 (V_2). As a result, it approaches the electrochemical oxidative potential of the analyte. The two peak potentials of a wave are distinguished by referring to the peak occurring at the positive potential sweep, the peak anodic potential (E_{pa}). The WE potential where the maximum current in a voltammetric analysis is received is called the peak potential (E_p). In the reverse cycle, the current decreases, the applied potential surpasses the E_p point, and the applied potential moves toward the negative values. In this case, the measured current turns into highly negative until reaching the electrochemical reductive potential of the analyte. Moreover, when the applied potential exceeds the E_p value, a peak polar to the anodic peak, named peak

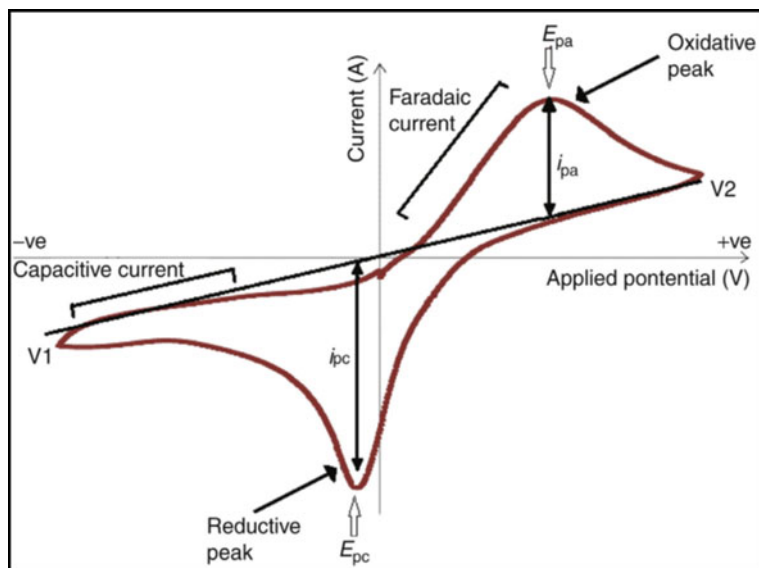


Fig. 7.3 Cyclic voltammogram presenting the peak cathodic potential (E_{pc}), peak anodic potential (E_{pa}), cathodic current (i_{pc}), and anodic current (i_{pa}). Reproduced (or adapted) with permission [8], © 2016, Elsevier

cathodic potential (E_{pc}), is formed and can be determined. Additionally, i_{pc} and i_{pa} are the differences between the cathodic and anodic currents from the resting current, respectively. While the process continues, the oxidative and reductive CV curves converge, indicating the reaction is nearing completion [8].

7.1.3 Advantages and Disadvantages of Cyclic Voltammetry

Cyclic voltammetry presents various advantages and a few main disadvantages. One of the advantages of CV is that it provides qualitative data about the features of electrochemical processes on electrode surfaces. Moreover, this technique yields significant data about the thermodynamics of oxidation–reduction and kinetics of adsorption processes, heterogeneous electron transfer, and coupled chemical reactions. This is possible since the researcher may conduct a reversible reaction in either direction [9, 10]. Different from other electrochemical methods, CV provides information through voltammograms. In addition, this method can characterize multiple species simultaneously under the condition that these species exhibit reduction and oxidation activity at different potentials. Furthermore, since pulse techniques were implemented, CV has achieved high sensitivity by deducing the influence of capacitive current [10]. Straightforward and largely accessible apparatus allow a simple operation condition [11].

Table 7.1 Advantages and disadvantages of CV

Advantages	Disadvantages
Provides qualitative data about the features of electrochemical processes on electrode surfaces [9, 10]	Indirect method [11]
Provides information about the thermodynamics of oxidation–reduction processes, kinetics of adsorption processes, and heterogeneous electron transfer and coupled chemical reactions [9, 10]	
Voltammograms offer extensive information [10]	Requires calibration for reliable data acquisition [11]
Capable of characterizing multiple species simultaneously [10]	
Simplicity of operation [11]	Molecules of same chemical class are challenging to differentiate [10]
High sensitivity [9]	
Cyclic voltammetry (CV)	

Some constraints of this technique are that it is an indirect characterization method and careful calibration is required for reliable data acquisition [11]. Moreover, alternative methods of CV occasionally have difficulties in discerning molecules that belong to the same chemical class. For instance, fast-scan cyclic voltammetry (FSCV) cannot differentiate dopamine, norepinephrine, and epinephrine as they are catecholamines that produce comparable voltammetric responses [10]. A summarized list of these advantages and disadvantages is found in Table 7.1.

7.1.4 Applications of Cyclic Voltammetry

Electrochemical techniques have been employed in order to identify a vast range of biomolecules. In combination with nanotechnology, they can develop low-cost, ultrasensitive, reliable, simple preparation routes, reproducible, portable, and easy-to-use devices. In electrochemical sensors, a biological event can be transformed into a quantifiable electrochemical signal, such as changes in current, impedance, and/or potential. The possibility of rapid and real-time detection makes this technology a potential tool for biosensing. A biosensor coupled with any electrochemical technique is able to quantify from small molecules to viruses in the order of nanometers [12]. For instance, miRNA is a biomarker that has recently been used for timely cancer detection. Modified graphene oxides with gold nanoparticles allowed the development of a device which detects miRNAs within plasma samples with great reproducibility and performance [13]. Another example is the fabrication of a biosensor using enzymes as biorecognition sites [14, 15]. The presence of high levels of uric acid can cause cardiovascular disease and hypertension, while low levels of it may lead to Alzheimer's disease. Cyclodextrins immobilized on carbon platforms allowed the electrochemical detection of uric acid with a detection threshold as small

as $0.06 \mu\text{M}$ [16]. Additionally, electropolymerized β -cyclodextrin on boron-doped reduced graphene oxide presented a limit of detection (LOD) of 0.6 nmol L^{-1} for flunitrazepam determination [17]. Another application of cyclodextrins is for the detection of spermine, a biomarker for cancer cells with a LOD of 0.001 mg L^{-1} which was achieved through benefiting from CV within an electrochemical setup [18].

The identification of protein biomarkers in the early stages of an illness could potentially pose a great challenge. Different cancer types including breast, ovarian, colon, and lung are associated with the serum protein called carcinoembryonic antigen (CEA). When the concentration of CEA is superior to 5 ng/ml , there is a high probability of developing a cancerous tumor. Timely detection of high CEA levels allows the individuals to receive appropriate attention, thus increasing the chances of preventing the disease. Conventional methods to identify CEA have drawbacks such as high costs, long response times, and complex procedures. Electrochemical techniques are attractive alternatives considering their portability, inexpensiveness, brief operation time, and ease of handling. Duy Thanh Tran et al. developed a sensing platform with high sensitivity and low DL for the electrochemical detection of CEA. This novel platform consisted of a combination of carbon nanotubes (CNTs) with microcarbon spheres (CSs) modified with copper–gold (Cu–Au) nanocrystals, and anti-CEA which was immobilized as a biorecognition site (Fig. 7.4a). The detection method was based on monitoring the oxidation–reduction reactions with potassium ferricyanide ($\text{K}_4 [\text{Fe}(\text{CN})_6]$) as a redox couple. When CEA interacts with the

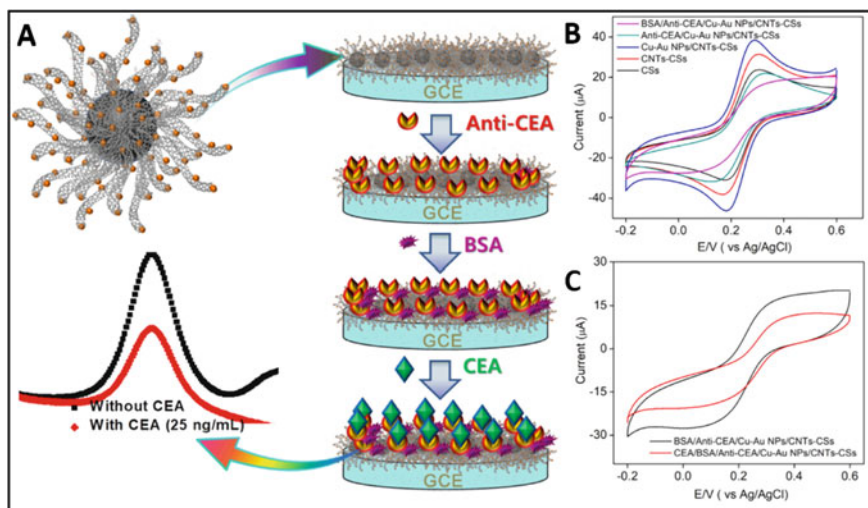


Fig. 7.4 a Fabrication of an electrochemical sensor for the identification of CEA. b CV curves of modified GCE in 0.1 M KCl with $5 \text{ mM K}_4[\text{Fe}(\text{CN})_6]$ at a scan rate of 50 mV s^{-1} and c CV curves of BSA/anti-CEA/Cu-Au NPs/CNTs-CSs modified GCE with and without 25 ng ml^{-1} of CEA in 0.1 M KCl containing $5 \text{ mM K}_4[\text{Fe}(\text{CN})_6]$ at a scan rate of 50 mV s^{-1} . Reproduced (or adapted) with permission [19], © 2018, Elsevier

sensing platform, the oxidation–reduction currents of the redox couple decreases. Figure 7.4b displays the electrochemical evaluation of each component present in the sensing platform and their effect on the performance of the redox reaction. The good electrical conductivity of the metal nanoparticles and the carbon structures favored the redox reaction, manifesting a hike in the peak currents of cathodic and anodic (blue and red lines). On the other hand, the presence of CEA and bovine serum albumin (BSA) on the platform surface decreased the electrochemical area, therefore affecting the performance of the redox couple (pink and green lines). The proposed sensing platform was successful in detecting CEA due to the decrease in peak currents associated with the redox couple in 25 ng ml^{-1} of CEA. The authors stated that CEA was adsorbed on the surface of the modified electrode forming an immunocomplex layer among CEA and anti-CEA (Fig. 7.4c) [19].

Dengue fever is a fatal disease that affects about 2.5 billion people which can further manifest into more acute phases such as dengue hemorrhagic fever (DHF) known as one of the most lethal symptoms. There are 4 different serotypes of dengue (DENV1, DENV2, DENV3, and DENV4) which could lead to dengue fever, and if not detected in time, may cause serious complications such as DHF or dengue shock syndrome (DSS). The flavivirus NS1 protein that circulates within the bloodstream from the starting point of the illness is utilized for the timely detection of dengue. Electrochemical sensors produce an electrical signal from a biological event, allowing the possibility of miniaturizing the system in a user-friendly, cost-effective, and portable fashion. Prima Dewi Sinawang et al. developed screen-printed gold electrode (SPGE) for the electrochemical detection of the NS1 protein where anti-dengue NS1 was immobilized, and polyethylene glycol (PEG)-stabilized was used as a biorecognition site. The species used to measure the electrochemical signal was the radical TEMPO (TEMPO•) (Fig. 7.5a). The authors explained the choice of this radical due to its solubility in water and the presentation of a well-defined electrochemical signal when the conjugated TEMPO• is on the gold nanoparticles (AuNPs). Subsequently, the authors developed an electro-lateral flow immunosensor (ELLI) device for NS1 detection using the SPGE modified with anti-dengue NS1 (Fig. 7.5b). The detection system was based on a sandwich immunoassay as follows: First, the synthesized immunonanoparticles (AuNPs–PEG–Ab–TEMPO•) were put in contact with the dengue NS1 protein present in the analyte. It was retained by the anti-dengue NS1, producing the first immunocomplex with electrochemical activity. Subsequently, the anti-dengue NS1 anchored on the SPGE surface captured the immunocomplex to complete the sandwich protocol. Thus, the anodic current associated with the oxidation of the TEMPO• radical in the sandwich was measured using CV. Dengue NS1 protein concentrations were selected from 0 ng ml^{-1} to 1000 ng ml^{-1} to obtain the calibration curves. A rise in the anodic current with the greater concentration of dengue NS1 protein was observed, which led the authors to claim that the system was capable of detecting dengue NS1 protein at concentrations higher than 50 ng ml^{-1} (Fig. 7.5c) [20].

Functionalization of the electrode surface increases the performance of electrochemical sensing devices considering that the inclusion of functional groups improves the surface interaction with the analyte of interest. Keita Nishimura et al.

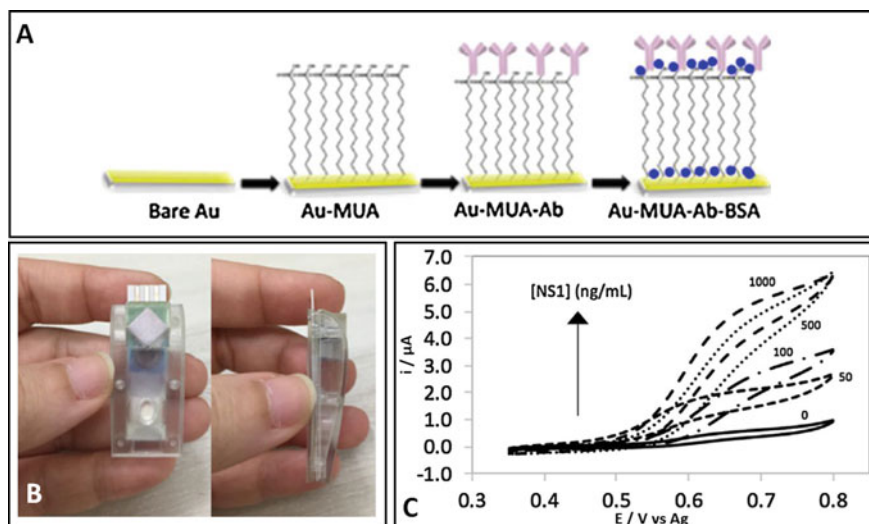


Fig. 7.5 a A schematic of the detailed procedure of screen-printed gold electrode (SPGE): gold (Au) surface, mercaptoundecanoic acid (MUA), and bovine serum albumin (BSA). b The electro-lateral flow immunosensor (ELLI) device. c Cyclic voltammograms of the detection of the NS1 protein over the lateral flow immunosensor by TEMPO• label on the formulation of electroactive immunonanoparticles. Reproduced (or adapted) with permission [20], © 2018, Elsevier

studied the effect of electrochemical functionalization with a 2 M sulfuric acid (H_2SO_4) solution on single-walled carbon nanotubes (SWNTs). The alterations in SWNTs morphology and electron transfer kinetics were evaluated, as well as the sensitivity changes in the detection of dopamine (DA). DA is a neurotransmitter that serves as a biomarker for Parkinson's disease and schizophrenia, in addition to being a stress marker. DA exhibits electrochemical activity by reversibly oxidizing to o-dopamine quinone (Fig. 7.6a). The authors stated that the current of the DA redox reaction increased at the functionalized electrode; hence, the sensitivity in DA detection also improved. This could be as a result of the functionalized surface impacting the electron transfer rate and the interaction between the electrode surface and the inner sphere redox species as with the DA (Fig. 7.6b) [21].

7.2 Electrochemical Impedance Spectroscopy for Material Characterization

7.2.1 History of Electrochemical Impedance Spectroscopy

Electrochemical impedance spectroscopy (EIS) is an electrochemical analytical method that can be utilized to observe biomolecular events at the surface of the

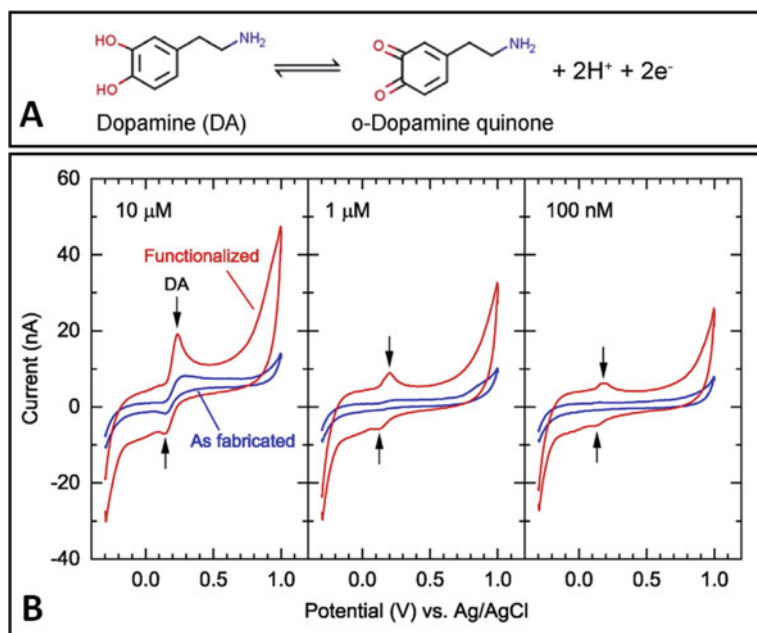


Fig. 7.6 **a** Redox reaction for dopamine. **b** Dopamine cyclic voltammograms obtained for as-fabricated and functionalized SWNTs with dopamine concentrations of (left) 10 μM, (middle) 1 μM, and (right) 100 nM. Reproduced (or adapted) with permission [21], © 2019, Elsevier

electrode through analyte interaction. EIS requires a large range of frequencies to measure the impedance properties of an electrochemical system. In comparison with other methods of biorecognition, electrochemical sensors are fast, portable, and cost effective [22, 23]. EIS was developed in 1894 by Oliver Heaviside, who coined the terms “impedance,” “admittance,” and “reactance” (Fig. 7.7). The origins of EIS date back to the late nineteenth century with the work of Heaviside, who introduced the linear systems theory (LST), formulated operational calculus, and established the operational impedance. In 1894, Walther Nernst measured the dielectric values of aqueous electrolytes and some organic fluids by means of the Wheatstone bridge. Later, in 1899, Emil Warburg extended the application of impedance to electrochemical systems by publishing an article on the impedance of diffusional transport of an electroactive species. In particular, the invention of the potentiostat in the mid-1900s and the introduction of frequency response analyzers in the 1970s were the major contributors to expansion of the field of EIS [22, 24, 25].

The implementation of EIS in electrochemical and corrosion mechanism research came to light when the potentiostat and the frequency response analyzer were developed as it enabled the examination of electrochemical interfaces at different frequencies and within the sub-millihertz range. The use of EIS was extended into biological systems by 1925 when Hugo Fricke obtained information of blood suspensions. Later, Kenneth Cole used EIS to collect data from urchin eggs and cell membranes

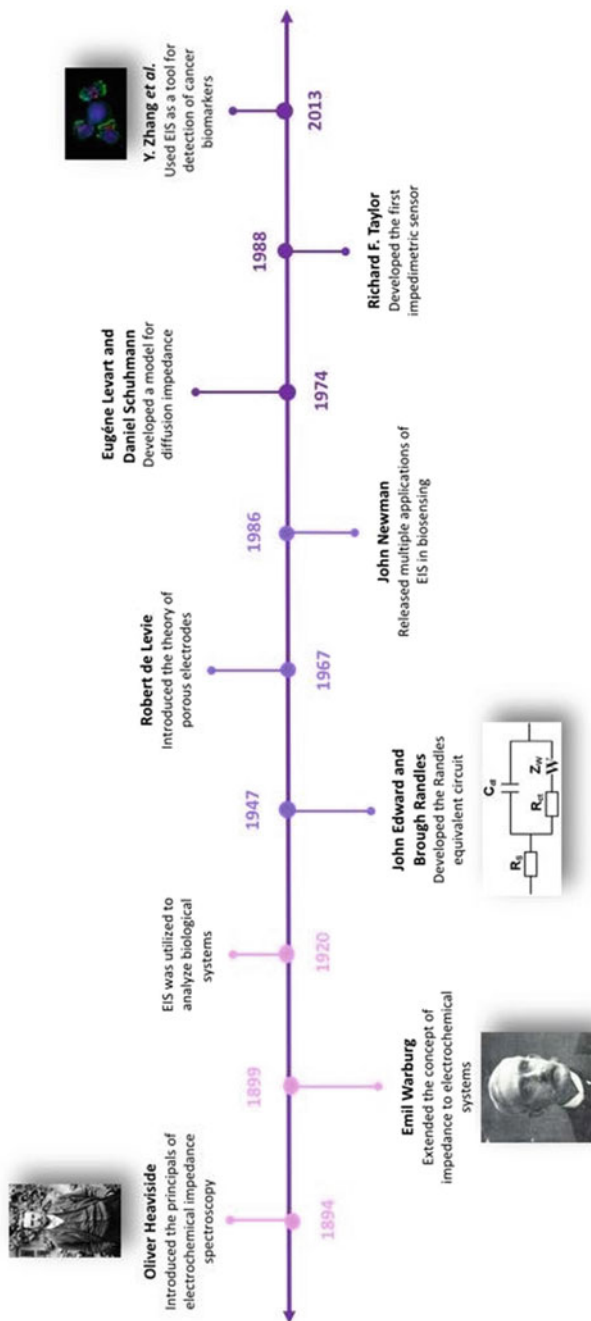


Fig. 7.7 History of EIS

(Fig. 7.7) [22, 24]. In 1947, John Edward Brough Randles developed Randles's equivalent circuit. This system facilitated the interpretation of EIS data obtained from solid interfaces. At a planar electrode, this circuit offers a pertinent simulation of the impedance characteristics of a fast charge transfer reaction. In 1967, Robert de Levie formulated transmission line models to calculate the impedance response of porous electrodes. Additionally, John Newman in 1970 demonstrated that high-frequency time-constant dispersion can result from the non-uniform current and potential distribution of disk electrodes. A few years later in 1974, Eugène Levart and Daniel Schuhmann created a framework for obtaining the diffusion impedance of a rotating disk considering the influence of homogeneous chemical reactions [22, 24, 25].

In 1988, the first impedimetric sensor was developed by Richard F. Taylor et al. Over the next few decades, the development of impedimetric biosensors has progressed. In 2004, Dianping Tang et al. created an electrode that enhanced the sensitivity of impedance measurements for hepatitis B detection [26]. Almost a decade later, Zhang et al. invented an EIS biosensor constructed on five screen-printed carbon electrodes coated with carboxyl-functionalized single-wall carbon nanotubes in order to identify a cancer biomarker [27]. An important step toward the development of an impedimetric biosensor was the immobilization of biomolecules; therefore, future advancements focused on enhancing operational stability, sensitivity, specificity, and resistance toward non-specific binding [27].

7.2.2 Mechanism of Operation of Electrochemical Impedance Spectroscopy

The concept of impedance in electronic devices is defined in the context of resistance. The basic principle of the electrochemical impedance method is to calculate how an electrode responds to a sinusoidal potential modulation for various frequencies. Regularly, common phenomena including alternating current (AC) modulations are applied to cathodic or anodic potential, or even to open-circuit potential. The numerical principles of electrochemical impedance rely on Ohm's law where the dependency of potential current for electrochemical systems is nonlinear [28]. However, in some cases, the cited dependence could be estimated between 5 and 10 mV; thus, the calculation of impedance is executed with an amplitude of 5–10 mV under a sinusoidal potential modulation. A sinusoidal current, $I(t)$, can be induced from sinusoidal perturbations of potential $E(t)$ with the equal frequency (ω). This frequency with the phase shift (ϕ) is superimposed onto the steady-state current according to the potential state. The definition of electrochemical impedance of electrode reaction (Z) is described similarly to Ohm's law for physical electric circuits. According to Eq. 7.1, E_0 is the amplitude of potential, I_0 is the current, and $\omega = 2\pi f$ is the radial frequency in rad/s (f is a frequency expressed in Hz).

$$Z(\omega) = \frac{E(t)}{I(t)} = \frac{|E_0| \sin \sin(\omega t)}{|I_0| \sin \sin(\omega t - \phi)} = Z_0 \frac{\sin \sin(\omega t)}{\sin \sin(\omega t - \phi)} \quad (7.1)$$

In a general sense, there are some components for the equivalent circuits of an electrochemical capacitor that maintain a capacitor connected to a resistance, an inductor, and an equivalent in series with a resistance. These are used to estimate the experimental impedance values with the distributed impedance elements, connected in series and/or in parallel. Impedance is the opposing force to electrical current in a circuit where its measurement unit is the same as resistance, ohms (Ω) [29]. Nevertheless, these differ considering resistance is defined as the opposition to the flow of electric current in the circuit, while impedance controls the flow of AC due to any components that are resistive, inductive, or capacitive. The key distinction between these two concepts is their behavior toward AC and direct current (DC). Under certain conditions, resistance can only be understood in an AC circuit: (a) The AC voltage is in phase with the current, (b) frequency independency is the main feature of the resistance, and (c) the resistance is applicable to all currents and voltages. As capacitive and/or inductive outcomes are noticeable with the majority of frequencies and the phase angle is not null in most cases, therefore resistance can be defined as the function of frequency.

Impedance demonstrates a quantitative concept of the opposition force to electrical current. A specified sinusoidal voltage is performed in the majority of EIS experiments by a potentiostat through a 3-electrode cell. This includes a solution of electrolyte harboring the researched molecule. The amplitude and load of the specified sinusoidal voltage are dependent on the type of molecular system of interest [30]. For instance, as the biological molecule structures are denatured, they are frequently influenced by smaller voltages than non-biological specimens. Another method for using EIS experiments within the biological applications is to functionalize the electrode surface. This would attract the analyte of interest to the surface of the electrode through an obstruction of a “molecularly wired” entrance process, thus affecting the conductivity of the system. After the composite and target analyte were immobilized on the electrode surface, impedance measurements can be conducted in a common redox probe (for instance, potassium ferricyanide (II), hexamine ruthenium (III) chloride, or a blank buffer solution) [31]. Consequently, when the load is conducted at a given frequency, a current will flow through the electrochemical cell which can be then obtained by the potentiostat. The registered flow current is converted by a software into an impedance measurement with an actual and predetermined element. The procedure would be duplicated for both components over a frequency range where different values are recorded [32].

As represented in Fig. 7.8a, in EIS experiments with potentiostat, the impulse is a small AC sine wave in the potential performed additionally to the DC potential. The behavior of the current to the electrochemical system includes an AC component translated into phase shifts from that of potential phase. The magnitude and phase of the AC mechanisms of the potential and current are considered as the phase. Additionally, kinetic information can be obtained from the magnitudes of the complex numbers $E \sim$ and $j \sim$. For example, their rate indicates the impedance of the circuit.

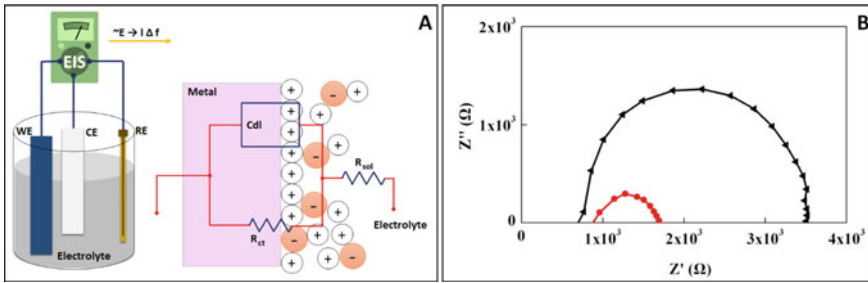


Fig. 7.8 **a** Illustration of the EIS test configuration. **b** Nyquist plot for a pure silicone-based material. Reproduced (or adapted) with permission [35], © 2014, American Physical Society

Experimentally, a function generator produces the small amplitude sine wave voltage (normally 5 mV rms), which is performed with a DC voltage in the electrochemical cell via a potentiostat. The reaction to this potential voltage is a current which overall contains both AC and DC components. The current is obtained through the current-to-voltage converter within the potentiostat or by calculating the voltage. Finally, a tool such as a frequency response analyzer (FRA) recognizes the amplitude and phase of the AC element of the current and the potential. Lastly, the amplitudes are converted into an impedance measure at the frequency of the sine wave which would be repeated at different frequencies in order to provide an impedance spectrum [33].

EIS spectra provide valuable information with respect to the electrochemical properties of the samples. The complex-impedance plane diagram, or Nyquist plot, maintains the polar plots and ensures the stability of the closed-loop control systems. In another word, the comprehensive frequency response of the open-loop transfer function is derived from Nyquist plots. It is common to plot $-Z_{\text{Im}}$ (also as $-Z''$ or $-Z_j''$) on the y-axis, which results in fitting data into the first quadrant of a graph. Even though the Nyquist plot is useful for recognizing the characteristic features of the system, the frequency information is inherently lost [34]. It is important to identify the frequencies of vital measurements such as superior and inferior real axis intercepts, and the characteristic frequency of an arc, ω_c . This value displays a peak $-Z_{\text{Im}}$ for a system. A Nyquist plot example is shown in Fig. 7.8b.

7.2.3 Advantages and Disadvantages of Electrochemical Impedance Spectroscopy

There are two main factors which draw specific attention to EIS: First, EIS data can be utilized to identify physical properties, such as diffusion coefficients, chemical reaction rates, and microstructural characteristics of the electrochemical system. Second, the execution of an EIS analysis is rather straightforward. Moreover, EIS is a versatile

technique that allows its application in a wide range of fields, including electrocatalysis and medicine [36]. Biomolecular events such as affinity interactions between peptides, receptors, nucleic acids, cells, and antibodies can occur at the surface of electrodes [23]. Such events, in turn, provide physical, chemical, and structural information of the surface at the micrometer scale [36]. Additionally, electric and dielectric properties of compounds under investigation can be obtained and analyzed using EIS [37]. Unlike other electrochemical techniques, EIS enables the measurement of the correlation between the current and applied voltage through the estimation of its transfer function within the frequency domain [36]. These measurements are possible for a wide range of frequencies, are characterized without requiring labels, and have high signal-to-noise ratio [23, 38, 39]. Rapid testing times, its sensitivity, ease of use, and non-destructive nature are among other known beneficial features of this technique (Table 7.2).

An important drawback of EIS is the ambiguity in the result interpretation. However, statistics and modeling can be implemented to overcome these issues [36]. Nonetheless, since the accuracy of the results depends on such fitting models, the ambiguity of the results can be aggravated [38]. An expensive instrumentation represents another limitation of EIS [39]. The application of EIS presents additional

Table 7.2 Advantages and disadvantages of electrochemical impedance spectroscopy

Advantages	Disadvantages
Wide range of applications, including the monitoring of biomolecular events at electrode surface [23, 36]	Susceptible to interpretation ambiguity [36]
Provides physical properties, chemical and microstructural information on surfaces [36]	
Provides information on electric and dielectric properties of samples [37]	Accuracy of results depends on fitting models [38]
Enables the estimation of the transfer function between current and applied voltage [36]	
Allows measurements at a wide range of frequencies [23, 38]	Expensive instrumentation [39]
Detection is label free [23]	
High SNR [23, 39]	Sensitive to surrounding environment thus requires Faraday cage [40]
Rapid test [38]	
Sensitivity [23]	Bulky experimental setups [40]
Ease of use [36]	
Non-destructive [37]	Requires theoretical simulation for data analysis [40]
Statistics and modeling can be used to overcome ambiguities in result interpretation [36]	
Signal-to-noise ratio (SNR)	

drawbacks, for instance, sensitivity to the surrounding environment, thus the need for a Faraday cage to mitigate noise. Moreover, the large experimental configurations and requiring theoretical simulation in order to analyze the data pose additional challenges [40].

7.2.4 *Applications of Electrochemical Impedance Spectroscopy*

The timely detection of diseases is a vital step for prevention and adequate treatments. EIS is an electrochemical technique that has been widely used in recent years as a detection tool considering it is easy to use, fast, and highly sensitive. The electrodes are modified/immobilized with biorecognition molecules that interact with the analytes of interest, hence altering the electrochemical response of the system. In this sense, the signal obtained could be attributed to (a) a non-faradaic process in which mainly the capacitance generated on the electrode/electrolyte interface is modified due to the interaction of the analyte with the surface of the modified electrode or (b) a faradaic process in which there is an electron transfer among a species present in the electrolyte and the modified electrode. The species that reacts electrochemically can be the analyte or a redox pair used indirectly by measuring the concentration of the analyte [23, 41, 42]. The advantages of EIS over other electrochemical techniques (e.g., CV) are that the biological species are not damaged during detection and the quantification signal is easy to obtain [43–45]. In addition, EIS allows the use of only two electrodes for detection, facilitating the fabrication of a laboratory on a chip (e.g., interdigitated electrodes) [46]. Some of the applications using non-faradic processes include the analysis of blood samples, detection of *E. coli* by aptamers, and detection of pre-osteoblast cells [47–49]. Moreover, biosensors based on faradaic processes for identification of the vascular endothelial growth factor, electrochemical detection of urea, cancer biomarkers, detection of NeutrAvidin, detection of active botulinum neurotoxin, and enzyme-based impedimetric biosensors are reported within the literature [50–56].

Lysozyme (concentration $\sim 0.5\text{--}2.0\text{ mg ml}^{-1}$ in mammals) is a protein that functions in the human body for anti-histaminic, anti-viral, anti-inflammatory, and anti-tumor activities. Changes in the concentration of this protein can refer to occurrence or progression of different illnesses including leukemia and meningitis indicated with an increase of lysozyme in urine or serum. Wei Chen et al. developed an electrode capable of identifying lysozyme in a simple and quick manner. The detection system consisted of a gold electrode modified with the anti-lysozyme aptamer (biorecognition site) and electrodeposited AuNPs to enhance electrical conductivity (Fig. 7.9a). EIS principals were used to monitor the presence of the lysozyme protein. The biomolecular receptor was immobilized on the Au surface and acts as a barrier for electron transfer and an electrical insulator. Consequently, if there was a redox couple in the analyte, the interaction between the protein and anti-protein will

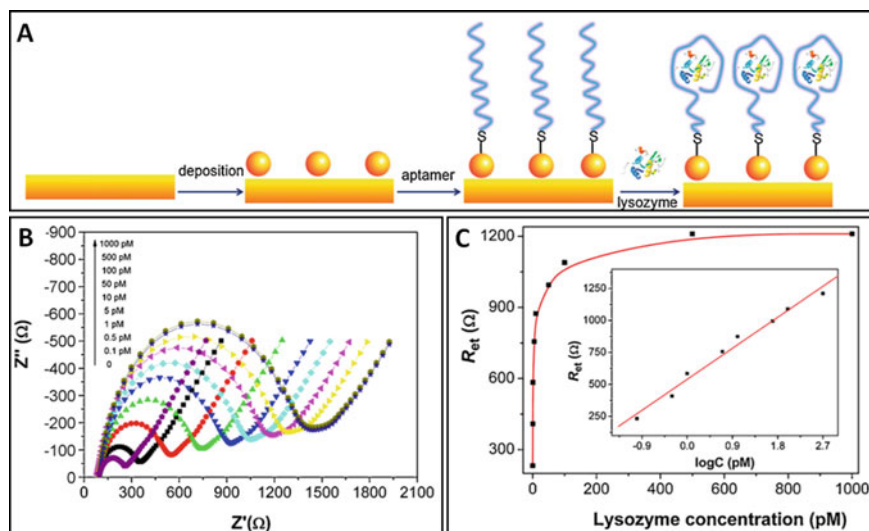


Fig. 7.9 **a** Illustration of an aptasensor with the procedure. **b** Nyquist plots of the aptamer/AuNPs/gold electrode following the interaction with a range of lysozyme concentrations between 0.1 and 500 pM. **c** The R_{et} dependence of the aptamer/AuNPs/gold electrode on the concentration of lysozyme. The inner graph presents a linear R_{et} with the logarithm of lysozyme concentration over the range of 0.1–500 pM. Reproduced (or adapted) with permission [43], © 2011, Elsevier

prevent the electrical transfer along the redox couple and the electrode. The Nyquist plots obtained at different concentrations of lysozine indicated how the resistance to electron transfer (R_{et}) increased with increasing protein concentration from 0.1 to 1000 pM (Fig. 7.9b). The calculated limit of detection (LOD) for this lysozyme aptasensor was 0.01 pM, and a linear trend of R_{et} with the logarithm of the protein concentration at the range of 0.1–500 pM resulted in an $R_{et} = 539.676 + 269.426 \log C$ (Fig. 7.9c) [43].

The development of efficient tools for the detection of tumor markers allows timely treatment of patients. An extracellular protein such as autocrine motility factor (AMF) stimulates the active migration of tumor cells and can be found in urine and blood serum. An important parameter in the motility of tumor cells is the interaction of AMF with its receptor AMFR/gp78 which has been associated with different types of cancer including prostate, breast, and bone among others. Devillers et al. presented an electrochemical biosensor based on F6P enzyme immobilization on gold (biorecognition phase) for the identification of a model protein named phosphoglucose isomerase (PGI) from rabbit muscle. EIS served as an electrochemical technique to indirectly detect the cancer biomarker AMF through the electrochemical activity of the redox couple. The authors used multiple concentrations from 10 fM to 100 nM of the model protein and observed in the Nyquist plots that increasing the enzyme concentration increased the resistance to electron transfer among the redox couple and the electrode surface (Fig. 7.10a). This behavior was attributed to the

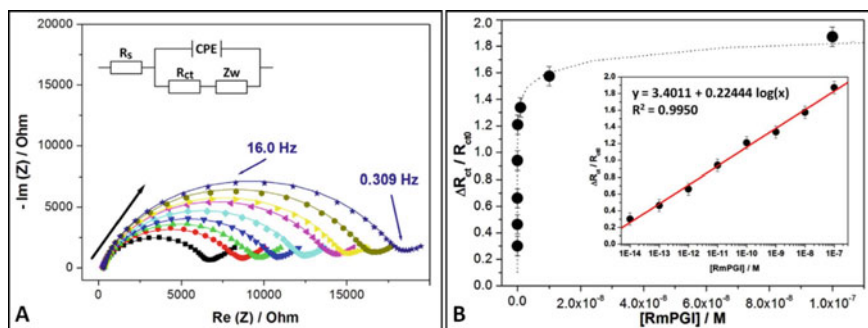


Fig. 7.10 **a** Nyquist plots of the PGI biosensor response (Black square: biosensor alone, Black circle: 10 fM, Black up-pointing triangle: 100 fM, Black down-pointing triangle: 1 pM, Black diamond: 10 pM, Black left-pointing pointer: 100 pM, Black right-pointing pointer: 1 nM, Black hexagon: 10 nM, Black star: 100 nM). **b** Calibration curve acquired from EIS data of the F6P biosensor in relation to the PGI concentration. Reproduced (or adapted) with permission [44], © 2017, Elsevier

fact that the interaction on the electrode surface among the F6P enzyme and the PGI protein prevents the redox couple from diffusing toward the electrode and reacting electrochemically. From the data obtained, the authors calculated a LOD of 6.6 fM over a range of PGI concentrations from 10 fM to 1 nM (Fig. 7.10b) [44].

Effective screening and capture of cancer cells aid patients to receive timely treatment and increase their chances of curing the disease. It is known that the concentration of folate receptor (FAR) correlates to the appearance of cancerous tumors; for example, ovarian tumors could present 34.31 pmol FAR/mg protein. Liping Du et al. developed an electrochemical biosensor for FAR-positive cells (HeLa cells) where the recognition site was folic acid immobilized on zirconium MOFs (UiO-66) using a gold electrode (Fig. 7.11a). The capture of HeLa cells on the surface of UiO-66 influences the system impedance since the characteristics of the electrode/electrolyte interface (e.g., resistance to electron transfer) are altered. When the concentration of the captured HeLa cells increased, the diameter of the semi-circle in the Nyquist plot also increased assuming the HeLa cells adhered to the surface of the modified electrode blocked the diffusion of the redox probe to the surface (Fig. 7.11b). The calculated LOD was 90 cells ml⁻¹ which was obtained from the changes in electron transfer resistance using Randles's equivalent circuit where Z_w is the Warburg impedance (diffusion redox probe), C is the capacitance (electrode/electrolyte interface), and R_s is the resistance to the solution (Fig. 7.11c) [45].

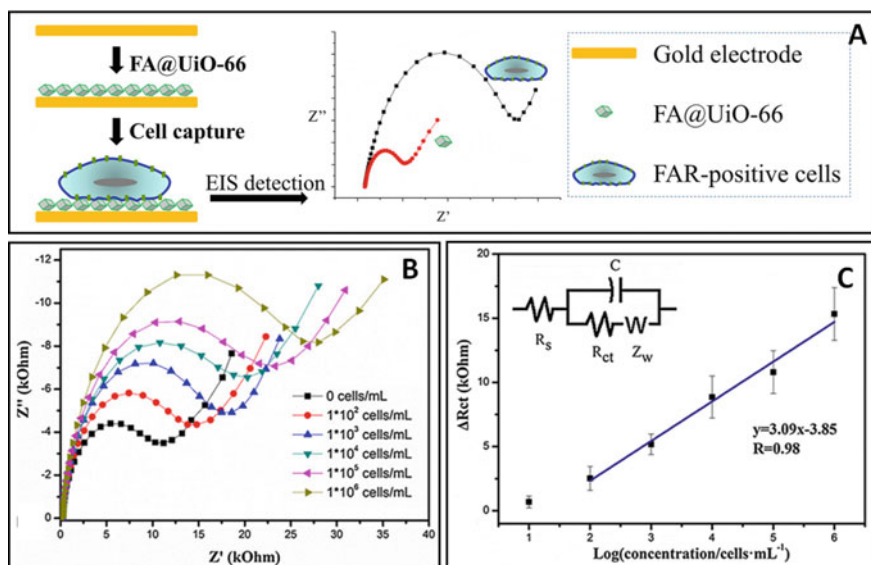


Fig. 7.11 a Elaboration of the FA@UiO-66-modified electrode to detect FAR-positive cells. b Nyquist plots of the gold electrode-functionalized FA@UiO-66 with various concentrations of HeLa cancer cells. c EIS calibration curves of FA@UiO-66-modified sensing electrodes; inside is the electrical equivalent diagram. Reproduced (or adapted) with permission [45], © 2019, Elsevier

7.3 Troubleshooting of Electrochemical Analysis Techniques

Voltammetry experiments measure the resulting current of an applied potential sweep on an electrochemical system. CV differs only in the fact that a linear potential is inversely increased once the linear potential sweep reaches the set value and subsequently returns to the initial potential [57, 58]. To perform a correct cyclic voltammetry experiment, the solvent and the analyte must be unreactive and must not be redox active in the selected scan window. Analytes can also be adsorbed to the electrode surface; therefore, before analyzing its reactivity, its homogeneity in solution should be assessed (Table 7.3) [57].

If the scan rate, the speed where the applied potential is scanned, is inadequately fast, it can lead to a voltammogram with no peak separations. This is due to the formation of a layer of the reduced analyte at the surface of the electrode, known as a diffusion layer [58]. The WE, which might be altered according to the experiment, is made from a redox-inert material. The desired electrochemical event occurs on its surface; thus, it is necessary to keep an extremely clean and well-defined area. Additionally, to ensure the kinetics of the reaction, it is important to have a greater surface area on the CE than the surface area of the WE (Table 7.3) [58].

The reference electrode must be maintained in good condition with an internal reference compound of a known potential. An issue that may present when using an

Table 7.3 Troubleshooting for characterization techniques used in electrochemical analysis

Technique	Problem	Cause	Solution
CV	Unseemly background scan [57]	Electrochemically active solution [57]	Verify that the scan window range is not electrochemically active for the solution [57]
		Impurities [57]	Polish the electrodes and glassware in order to recreate the solution [57]
	No peak-to-peak separation [58]	Surface-adsorbed species [58]	Increase scan rates [58]
	Distortion of the voltammogram [58]	WE surface contamination [58]	Electrode's surface should be polished (according to the type of electrode), or it can be subjected to removing particles [58]
			CV scans in simple electrolyte are also necessary to remove species [58]
Increased peak-to-peak separation in the voltammogram in an electrochemically reversible experiment [58]	Ohmic drop [58]	Reduce the size of the WE to decrease the current or use low scan rates [58]	
		Increase the electrolyte concentration [58]	
		Place the working and reference electrode closer [58]	
EIS	Unclear interpretation of the resulting spectra [25]	Non-uniform current flow [25]	Use an electrode where the current and potential distribution is constant [25]
	Signal-to-noise ratio, stochastic errors [25]	Selection of experimental parameters [25]	Increase integration time at each frequency as many cycles as required [25]
			Increase the modulation amplitude [25]
Error in the impedance response [25]	Transient [25]	Apply a one- or two-cycle delay between the change of frequency and impedance measurement [25]	
		Disregard the first obtained frequency when applying regression techniques [25]	

CV Cyclic voltammetry; EIS electrochemical impedance spectroscopy; WE working electrode

AgCl/Ag electrode is the silver ion (Ag^+) leakage into the rest of the analyte solution which could lead to interference with the electrochemical measurements [58]. An inert atmosphere should be prepared at the assembled cell. Due to the electrochemical response of analytes, these can be altered by the presence of oxygen; thus, the electrolyte solution should be treated with an inert gas before the electrochemical experiment (Table 7.3) [57, 58].

Optimization of the parameter for EIS settings maximizes the values of the obtained spectrum. However, the parameter settings may be inapplicable to all impedance devices [25]. In impedance measurements, each frequency involves the transition of time-domain signals to a complex value. Therefore, if the integration time at each frequency is increased, the chances of errors can be minimized as well. The number of cycles required for every frequency, in turn, corresponds to the number of the calculation [25]. For systems that have a broad range of potential, the non-arbitrary miscalculations may be greatly mitigated by means of a wide adjustment amplitude. Another error in impedance measurements is a transient that could be observed in the change from one frequency to another; therefore in the difference between the frequency and impedance, a delay of one or two cycles is recommended. Additionally, a start-up transient might corrupt the first frequency of measurement; thus, it is suggested to ignore the first measurement (Table 7.3) [25]. Table 7.3 offers a number of possible errors when dealing with electrochemical characterizations of a sample, the possible causes, and the recommended solutions to address such problems.

References

1. K. Lubert, History of Electroanalytical Methods, pp. 1937–1946 (2010). <https://doi.org/10.1002/elan.201000087>
2. A.J. Bard, C.G. Zoski, Voltammetry retrospective. *Anal. Chem.* 346–352 (2000)
3. J.M. Díaz-cruz, N. Serrano, C. Pérez-ràfols, C. Ariño, M. Esteban, Electroanalysis from the Past to the Twenty-First Century : Challenges and Perspectives, pp. 2653–2661 (2020)
4. C. Batchelor-mcauley, E. Kätelhçn, E.O. Barnes, R.G. Compton, E. Laborda, A. Molina, Recent Advances in Voltammetry, pp. 224–260 (2015). <https://doi.org/10.1002/open.201500042>
5. M. Armstrng-james, J. Millar, Carbon fibre microelectrodes. *J Neurosci. Methods* **1**, 279–287 (1979)
6. D. Guziejewski, Electrode mechanisms with coupled chemical reaction—Amplitude effect in square-wave voltammetry. *J. Electroanal. Chem.* **870**, 114186 (2020). <https://doi.org/10.1016/j.jelechem.2020.114186>
7. F. Harnisch, S. Freguia, A basic tutorial on cyclic voltammetry for the investigation of electroactive microbial biofilms. *Chem. Asian J.* **7**(3), 466–475 (2012). <https://doi.org/10.1002/asia.201100740>
8. O. Guy, K. Walker, -Silicon carbide biotechnology, and undefined 2016, in Graphene Functionalization for Biosensor Applications. Elsevier
9. J. Hoyos-Arbeláez, M. Vázquez, J. Contreras-Calderón, Electrochemical methods as a tool for determining the antioxidant capacity of food and beverages: A review. *Food Chem.* **221**, 1371–1381 (2017). <https://doi.org/10.1016/j.foodchem.2016.11.017>
10. J.G. Roberts, L.A. Sombers, Fast-scan cyclic voltammetry: Chemical sensing in the brain and beyond. *Anal. Chem.* **90**(1), 490–504 (2018). <https://doi.org/10.1021/acs.analchem.7b04732>

11. J. Sworakowski, How accurate are energies of HOMO and LUMO levels in small-molecule organic semiconductors determined from cyclic voltammetry or optical spectroscopy. *Synth. Met.* **235**, 125–130 (2018). <https://doi.org/10.1016/j.synthmet.2017.11.013>
12. J.R. Anusha, B. Chul, K. Yu, C.J. Raj, Electrochemical biosensing of mosquito-borne viral disease, dengue : A review. *Biosens. Bioelectron.* **142**(June), p. 111511 (2019). <https://doi.org/10.1016/j.bios.2019.111511>
13. M. Azimzadeh, M. Rahaie, N. Nasirizadeh, K. Ashtari, H. Naderi-manesh, An electrochemical nanobiosensor for plasma miRNA-155, based on graphene oxide and gold nanorod, for early detection of breast Cancer. *Biosens. Bioelectron.* (2016). <https://doi.org/10.1016/j.bios.2015.09.020>
14. C. Pan, H. Wei, Z. Han, F. Wu, L. Mao, Enzymatic electrochemical biosensors for in-situ neurochemical measurement. *Curr. Opin. Electrochem.* (2019). <https://doi.org/10.1016/j.coelec.2019.12.008>
15. J. Yoon et al., Flexible electrochemical glucose biosensor based on GOx/gold/MoS₂/gold nano film on the polymer electrode. *Biosens. Bioelectron.* **140**(May), p. 111343 (2019). <https://doi.org/10.1016/j.bios.2019.111343>
16. K.P. Aryal, H.K. Jeong, Functionalization of β -cyclodextrin into ambient plasma modified carbon nanotube-thermally reduced graphite oxide for electrochemical sensing of uric acid. *Mater. Chem. Phys.* **238**(July), 121899 (2019). <https://doi.org/10.1016/j.matchemphys.2019.121899>
17. M. Hossein, Z. Norouzi, M. Mahdi, Using a nanocomposite consist of Boron-doped reduced graphene oxide and electropolymerized β -cyclodextrin for Flunitrazepam electrochemical sensor. *Microchem. J.* **156**(May), 104994 (2020). <https://doi.org/10.1016/j.microc.2020.104994>
18. S. Shrivastava, P. Kumar, N. Verma, Spermine biomarker of cancerous cells voltammetrically detected on a poly (β -cyclodextrin)—electropolymerized carbon film dispersed with Cu—CNFs. *Sensors Actuators B. Chem.* **313**(January), 128055 (2020). <https://doi.org/10.1016/j.snb.2020.128055>
19. D. Thanh, V.H. Hoa, L. Huu, N. Hoon, J. Hee, Cu-Au nanocrystals functionalized carbon nanotube arrays vertically grown on carbon spheres for highly sensitive detecting cancer biomarker. *Biosens. Bioelectron.* **119**(July), 134–140 (2018). <https://doi.org/10.1016/j.bios.2018.08.022>
20. P. Dewi, L. Fajs, K. Elouarzaki, J. Nugraha, R.S. Marks, Chemical TEMPO-based immunolateral flow quantitative detection of dengue NS1 protein. *Sensors Actuators B. Chem.* **259**, 354–363 (2018). <https://doi.org/10.1016/j.snb.2017.12.043>
21. K. Nishimura, T. Ushiyama, N. Xuan, M. Inaba, S. Kishimoto, Y. Ohno, Enhancement of the electron transfer rate in carbon nanotube flexible electrochemical sensors by surface functionalization. *Electrochim. Acta* **295**, 157–163 (2019). <https://doi.org/10.1016/j.electacta.2018.10.147>
22. J.V. Rushworth, A. Ahmed, P.A. Millner, D.J. Pike, N.A. Hirst, J.A. Goode, *Impedimetric Biosensors for Medical Applications: Current Progress and Challenges*. Momentum Press, New York [New York] (2013)
23. L.G. Zamfir, M. Puiu, C. Bala, Advances in electrochemical impedance spectroscopy detection of endocrine disruptors. *Sensors (Switzerland)* **20**(22), 1–21 (2020). <https://doi.org/10.3390/s20226443>
24. D.D. MacDonald, Reflections on the history of electrochemical impedance spectroscopy. *Electrochim. Acta* **51**(8–9), 1376–1388 (2006). <https://doi.org/10.1016/j.electacta.2005.02.107>
25. M. Orazem, B. Tribollet, *Impedance Spectroscopy* (2008)
26. D. Tang, R. Yuan, Y. Chai, J. Dai, X. Zhong, Y. Liu, A novel immunosensor based on immobilization of hepatitis B surface antibody on platinum electrode modified colloidal gold and polyvinyl butyral as matrices via electrochemical impedance spectroscopy. *Bioelectrochemistry* **65**(1), 15–22 (2004). <https://doi.org/10.1016/j.bioelechem.2004.05.004>
27. A.J. Tkac et al., Electrochemical impedance spectroscopy-based biosensors: Mechanistic principles, analytical examples for assay of protein cancer biomarkers and challenges towards commercialization. *Chem. Electro Chem.* <https://doi.org/10.1002/celec.201800848>

28. "The Study of Thin Films by Electrochemical Impedance...—Google Scholar."
29. "C. Alexander and M. Sadiku, Fundamentals of Electric...—Google Scholar."
30. B. Hirschorn, I. Ibrahim, M.E. Orazem, H. Takenouti, B. Tribollet, Effect of large perturbation amplitudes on the impedance response of an electrochemical system. *ECS Trans.* **13**(13), 81–100 (2019). <https://doi.org/10.1149/1.3004031>
31. E.P. Randviir, D.A.C. Brownson, D.K. Kampouris, Electrochemistry of Q-graphene carbon dioxide utilisation view project lithium-ion battery view project. *pubs.rsc.org*. <https://doi.org/10.1039/c2nr31823g>
32. E.P. Randviir, C.E. Banks, E.P. Randviir, Electrochemical Impedance Spectroscopy: An Overview of Bioanalytical Applications. *pubs.rsc.org*. <https://doi.org/10.1039/c3ay26476a>
33. D.A. Harrington, Electrochemical Impedance Spectroscopy. Norwegian University of Science and Technology (NTNU) (2004)
34. M. Orazem, B.T.-N. Jersey, Electrochemical impedance spectroscopy. *iopscience.iop.org* (2008)
35. Y. Liu et al., Percolation mechanism through trapping/de-trapping process at defect states for resistive switching devices with structure of Ag/SixCl–x/p-Si Percolation mechanism through trapping/de-trapping process at defect states for resistive switching devices with. *Artic. J. Appl. Phys.* **116**(6), 64505 (2014). <https://doi.org/10.1063/1.4893016>
36. F. Ciucci, Modeling electrochemical impedance spectroscopy. *Curr. Opin. Electrochem.* **13**, 132–139 (2019). <https://doi.org/10.1016/j.coelec.2018.12.003>
37. J. Qi, G.E. Thompson, Comparative studies of thin film growth on aluminium by AFM, TEM and GDOES characterization. *Appl. Surf. Sci.* **377**, 109–120 (2016). <https://doi.org/10.1016/j.apsusc.2016.03.115>
38. C. Pastor-Fernández, K. Uddin, G.H. Chouchelamane, W.D. Widanage, J. Marco, A comparison between electrochemical impedance spectroscopy and incremental capacity-differential voltage as Li-ion diagnostic techniques to identify and quantify the effects of degradation modes within battery management systems. *J. Power Sources* **360**, 301–318 (2017). <https://doi.org/10.1016/j.jpowsour.2017.03.042>
39. D. Harrington, Chapter 1. Introduction, in *Electrochemical Impedance Spectroscopy* (2004), pp. 1–12
40. G. Luka et al., Microfluidics Integrated Biosensors: A Leading Technology towards Lab-on-a-Chip and Sensing Applications. *mdpi.com* (2015). <https://doi.org/10.3390/s151229783>
41. S. Brosel-oliu, N. Abramova, N. Uria, A. Bratov, Analytica Chimica Acta Impedimetric transducers based on interdigitated electrode arrays for bacterial detection e A review. *Anal. Chim. Acta* (xxxx) (2019). <https://doi.org/10.1016/j.aca.2019.09.026>
42. A. Chakraborty, D.N. Tibarewala, A. Barui, 5. Impedance-Based Biosensors. Elsevier Ltd (2019)
43. Z. Chen, L. Li, H. Zhao, L. Guo, X. Mu, Electrochemical impedance spectroscopy detection of lysozyme based on electrodeposited gold nanoparticles. *Talanta* **83**(5), 1501–1506 (2011). <https://doi.org/10.1016/j.talanta.2010.11.042>
44. M. Devillers, L. Ahmad, H. Korri-Youssofi, L. Salmon, Carbohydrate-based electrochemical biosensor for detection of a cancer biomarker in human plasma. *Biosens. Bioelectron.* **96**(January), 178–185 (2017). <https://doi.org/10.1016/j.bios.2017.04.031>
45. L. Du, W. Chen, J. Wang, W. Cai, S. Kong, C. Wu, Folic acid-functionalized zirconium metal-organic frameworks based electrochemical impedance biosensor for the cancer cell detection. *Sensors Actuators, B Chem.* **301**(June), 127073 (2019). <https://doi.org/10.1016/j.snb.2019.127073>
46. A.Z. Murad, Interdigitated Electrodes as Impedance and Capacitance Biosensors: A Review, vol. 020276 (2017). <https://doi.org/10.1063/1.5002470>
47. S. Analysis, Interdigitated Sensor Optimization for Blood Sample Analysis (2020)
48. G.N. Abdelrasoul et al., Analytica Chimica Acta DNA aptamer-based non-faradaic impedance biosensor for detecting. *Anal. Chim. Acta* **1107**, 135–144 (2020). <https://doi.org/10.1016/j.aca.2020.02.004>

49. A.G. Montaño-figueroa, S.E. Wheelis, B.M. Hedden, N.H. Alshareef, Detection of apoptotic and live pre-osteoblast cell line using impedance- based biosensors with variable electrode design. *Biosens. Bioelectron.* **128**(December 2018), 37–44 (2019). <https://doi.org/10.1016/j.bios.2018.11.057>
50. M. Kim, R. Iezzi Jr., B.S. Shim, D.C. Martin, Impedimetric Biosensors for Detecting Vascular Endothelial Growth Factor (VEGF) Based on (PEDOT)/Gold Nanoparticle (Au NP) Composites, vol. 7, no. April, pp. 1–11 (2019). <https://doi.org/10.3389/fchem.2019.00234>
51. F.L. Migliorini, R.C. Sanfelice, L.A. Mercante, R.S. Andre, L.H.C. Mattoso, D.S. Correa, Urea impedimetric biosensing using electrospun nanofibers modified with zinc oxide nanoparticles. *Appl. Surf. Sci.* **443**, 18–23 (2018). <https://doi.org/10.1016/j.apsusc.2018.02.168>
52. N.I. Khan, A.G. Maddaus, E. Song, A Low-Cost Inkjet-Printed Aptamer-Based Electrochemical Biosensor for the Selective Detection of Lysozyme (2018). <https://doi.org/10.3390/bios8010007>
53. L. Han, P. Liu, A.P. Valery, A. Liu, A label-free electrochemical impedance cytosensor based on specific peptide-fused phage selected from landscape phage library. *Nat. Publ. Gr.* (October 2015), 1–10 (2016). <https://doi.org/10.1038/srep22199>
54. B. Hong, A. Sun, L. Pang, A.G. Venkatesh, D. Hall, Y. Fainman, Integration of Faradaic Electrochemical Impedance Spectroscopy into a Scalable Surface Plasmon Biosensor for in Tandem Detection, vol. 23, no. 23, pp. 813–820 (2015). <https://doi.org/10.1364/OE.23.030237>
55. J. Halliwell, A.C. Savage, N. Buckley, C. Gwenin, Electrochemical impedance spectroscopy biosensor for detection of active botulinum neurotoxin. *Sens. Bio-Sensing Res.* **2**, 12–15 (2014). <https://doi.org/10.1016/j.sbsr.2014.08.002>
56. J. Guan, Y. Miao, Q. Zhang, Impedimetric Biosensors, vol. 97, no. 4, pp. 219–226 (2004)
57. JoVE Science Education Database, Analytical chemistry. Cyclic Voltammetry (CV). JoVE, Cambridge, MA (2021)
58. K.J. Rountree, B.D. Mccarthy, E.S. Rountree, T.T. Eisenhart, J.L. Dempsey, A Practical Beginner’s Guide to Cyclic Voltammetry (2017). <https://doi.org/10.1021/acs.jchemed.7b00361>